Advances in Real-Time Non-Contact Monitoring of Medical Thermal Treatment Through Multistatic Array Microwave Imaging

John Stang, *Member, IEEE,* Guanbo Chen, *Student Member, IEEE,* Mark Haynes, *Member, IEEE,* and Mahta Moghaddam, *Fellow, IEEE*

***Abstract*—In this paper, we present some recent advances in real-time non-contact monitoring of thermal treatment through multistatic array imaging. The work presented was primarily motivated by the need to improve the flexibility and computational efficiency of the forward modeling of microwave imaging systems in general and of our real-time microwave thermal monitoring system in particular. Specifically, we have developed a conformal finite-difference time domain (CFDTD) solver that addresses several limitations inherent to our previously reported forward modeling methods. In particular, this CFDTD solver has enabled the implementation of a fully integrated numerical vector Green's function that addresses the task of linking the object's scattered field to the measured scattered voltage in a more general and flexible way than the waveport vector Green's function method used in our earlier work. Both the CFDTD solver and the integrated numerical Green's function are validated for a prototype microwave imaging cavity through comparison with CST Microwave Studio. These validated methods are currently being used in an ongoing experimental characterization of microwave imaging for both dielectric reconstruction and real-time thermal monitoring.**

I. Introduction

THERMAL therapy is a fast-growing and increasingly versatile category of treatments in the fight against cancer. Researchers have developed a number of methods (both invasive and noninvasive) to deliver thermal energy in a variety of forms (including ultrasound, radiofrequency, microwave, and laser). Common to all of these thermal therapies, however, is the necessity for real-time thermal monitoring and guidance, and the current standard of MRI-based thermal monitoring is cumbersome, expensive, and requires the therapy system design to be MR-compatible.

As a potential alternative to MR-based thermal monitoring, a prototype real-time noninvasive thermal monitoring system based on multistatic microwave imaging was developed [1]. This system used microwaves to detect the small changes in the complex permittivity of water that occur due to changes in temperature, and built upon methods [2] and hardware [3] developed previously for the application of breast cancer screening. The inversion algorithm, control hardware, and measurement hardware were optimized for real-time image formation (refresh rates better than 1 frame per second), and the system was validated with heating tests in simple phantoms.

During the process of developing and experimentallly validating the prototype system, it became apparent that improvements in the flexibility and computational efficiency of the forward modeling would be necessary before real-time thermal imaging would be clinically viable. To address these limitations, we have developed an in-house wideband forward solver that integrates (a) object modeling (b) waveport excitation, and (c) S-parameter extraction under a conformal finite difference time domain (CFDTD) framework. In particular, this CFDTD solver has enabled the implementation of a fully integrated numerical vector Green's function that addresses the task of linking the object's scattered field to the measured scattered voltage in a more general and flexible way than the waveport vector Green's function method used in our earlier work. In this paper, we show how these methods fit into the larger context of multistatic microwave imaging for real-time thermal monitoring, give an overview of the development of both the CFDTD solver and the integrated numerical Green's function, and demonstrate their use in the successful modeling of a prototype microwave imaging cavity with validation through comparison with results from CST Microwave Studio.

II. Methods

A. Dual Application of Microwave Imaging to Real-Time Thermal Monitoring

Real-time microwave monitoring of thermal treatments is based upon two fundamental assumptions: knowledge of the complex dielectric properties of the tissue in the region of interest prior to heating and knowledge of how the dielectric properties of each tissue type will change as a function of temperature. One method of obtaining these dielectric properties is to infer them from an earlier imaging study (such as MRI). However, this has the potential to introduce error both from inaccuracies in mapping one material property (typicallly water content) to another (complex permittivity) and from uncertainty in coregistering the earlier imaging study with the current patient geometry during the thermal therapy procedure. Instead, it is preferable to generate a map of the dielectric properties directly using the same microwave imaging system used for real-time monitoring, and it is

J. Stang, G. Chen, and M. Moghaddam are with the Department of Electrical Engineering - Electrophysics, University of Southern California, Los Angeles, CA, 90089 USA e-mail: (see http://mixil.usc.edu/).

M. Haynes is with the Jet Propulsion Laboratory, Pasadena, CA 91109.

Manuscript submitted November 4,2015.

978-1-4673-9149-8/15/$31.00 ©2015 IEEE

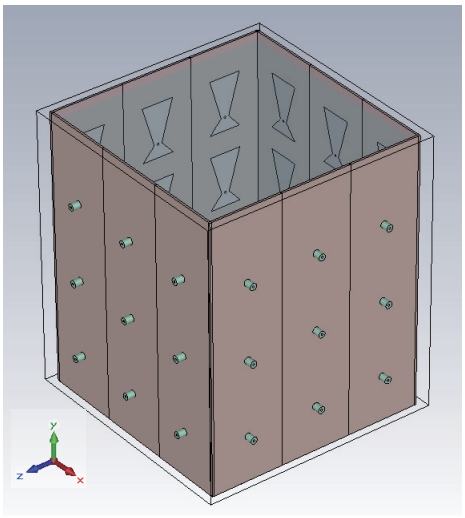

Fig. 1: CAD Drawing of Prototype Imaging Cavity

specifically for this task that the conformal finite-difference time domain (CFDTD) forward solver discussed in this paper has been developed and integrated into the inversion algorithm shown in flow chart form in Figure 2. The iterative inversion algorithm outlined in the figure uses the following procedure:

1. In the absence of the object, use the conformal FDTD method to calculate the incident field inside the object region for each antenna.

2. Use the incident field due to antenna M and the total field due to antenna N to construct a numerical Greens function linking the unknown object material property to the scattered S-parameter S_{MN} in the presence of the imaging cavity and object. (Note: in the first iteration, the incident field is substituted for the total field in the object region.)

3. Solve for the object material using the local optimization method with regularization and then use this solution to update the material properties in the object region.

4. With the updated object material, use the conformal FDTD method to calculate the total field in the object region and the scattered field in the antenna feed.

5. Compare the difference between the measured and FDTD-calculated scattered fields at the antenna feed. If the difference is smaller than the threshold, stop, and output estimated map of complex permittivity. Otherwise, return to step 2 with the updated total field in the object region.

With the volumetric map of the complex permittivity from the inversion alogrithm and the corresponding electric fields from the CFDTD solver in hand, it is then possible to use the Distorted Born Approximation and precompute a linear inverse scattering solution that can be applied in real-time to the multistatic scattered S-parameter measurements that are being continuously acquired by the real-time microwave imaging hardware. This solution, combined with the aforementioned knowledge of how complex permittivity varies with temperature for a given tissue type is what enables real-time thermal monitoring via multistatic array microwave imaging.

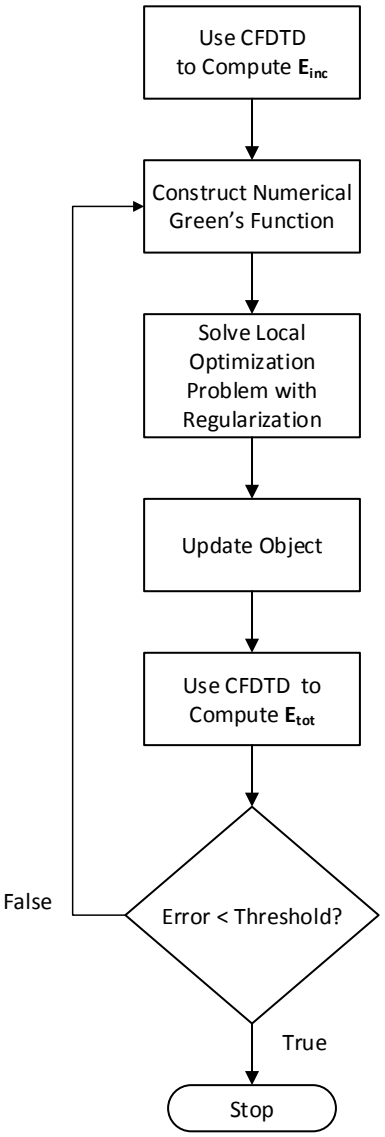

Fig. 2: Inversion Flow Chart with CFDTD Forward Solver and Integrated Numerical Green's Function.

B. Conformal FDTD Solver with Waveport Excitation and S-Parameter Extraction

From its initial conception by Yee [4], to the development of modern commercial packages, the finite-difference time domain (FDTD) method has proven an increasingly useful tool in the modeling of electromagnetic problems. Along the way, researchers have made a variety of evolutionary improvements designed to address issues of computational efficiency, robustness, and accuracy. Among the most significant of these was the development of the conformal FDTD (CFDTD) method [5], which utilizes the fact that the E and H fields are not collocated within one Yee cell and creates an effective material that captures the geometry of curvilinear objects without the need for the dense meshing required by the traditional staircase Yee grid.

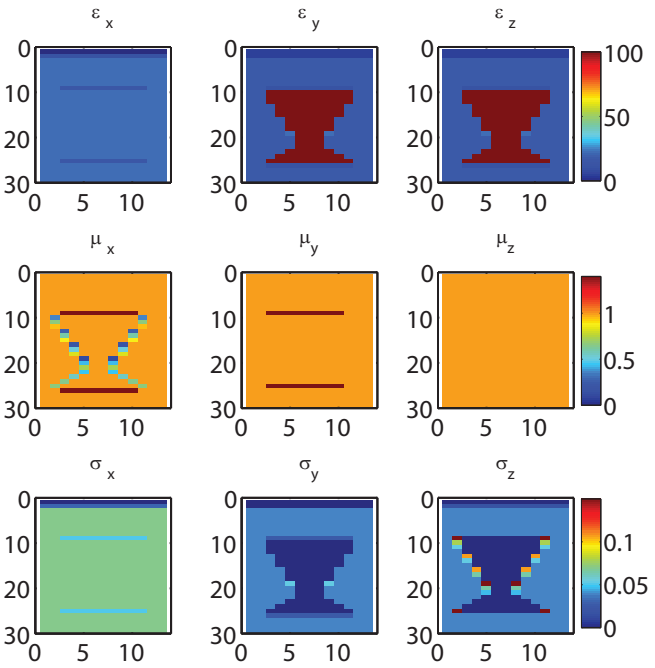

Fig. 3: Effective Materials (Row 1: ϵ, Row 2: μ, Row 3: σ) Used to Model Antennas in Imaging Cavity with CFDTD

In order for the CFDTD method to be practically useful in the forward modeling of multistatic antenna array measurements, however, two additional modeling challenges must be addressed: **(1)** how to model the source excitation at the antenna feed, and **(2)** how to determine the transmit and receive voltages in the feed to extract the S-parameters representing the actual measured signal. Toward that end, a CFDTD forward solver has been developed that integrates **(1)** a conformal 2D finite-difference frequency domain (FDFD) solver to calculate the field distribution and propagation constant of the waveport and a total field scattered field (TFSF) based soft source to feed that solution into the waveport, and **(2)** an S-parameter extraction method compatible with the conformal framework. Full details of this implementation are beyond the scope of this paper, but have been submitted for publication in *IEEE Trans. on Antennas and Propagation* [7].

C. Integrated Numerical Vector Green's Function

Numerical Green's functions, such as the one introduced by Yuan and Liu [6], are used in microwave imaging to account for the effects of the antenna pattern and the presence of the imaging cavity and to link the measured scattered voltage to the object's scattered field during the inversion process. Haynes et al. [2] introduced a waveport vector Green's function which proved highly effective in accounting for the various nonidealities of real antennas radiating into an imaging cavity, and enabled the development of an experimentally validated imaging system [3]. However, this method relies on inputs from an external forward solver to model the electric fields. Since this requires passing the electric field data from the external solver to the vector Green's implementation in the inversion algorithm, it is inherently cumbersome and computationally inefficient. Furthermore, limitations of the forward solver (in [3], the commercial finite element solver, HFSS) also limited the vector Green's function to the background case (Born Iterative type) or to very simple objects (Distorted Born type). To address these limitations, we introduce a numerical vector Green's function that is directly integrated into the conformal FDTD forward solver discussed in the previous section.

Derivation of Numerical Vector Green's Function from the Reciprocity Principle: Using reciprocity, we have:

$$\int_V \boldsymbol{E}_{scat}(\boldsymbol{r}) \cdot \boldsymbol{J_s}(\boldsymbol{r}) dv = \int_{V'} \boldsymbol{E}_{inc}(\boldsymbol{r'}) \cdot \boldsymbol{J}_{pol}(\boldsymbol{r'}) dv' \tag{1}$$

where $\boldsymbol{r}$ is at the antenna feed, $\boldsymbol{r'}$ is at the object region, $\boldsymbol{E}_{scat}$ is the scattered field produced by the polarization current $\boldsymbol{J}_{pol}$ and $\boldsymbol{E}_{inc}$ is the incident field produced by the test point current source $\boldsymbol{J_s}$. The polarization current produced by the object contrast and the total fields in the object region when transmitted from antenna N can be represented as,

$$\boldsymbol{J}^N_{pol}(\boldsymbol{r'}) = j\omega\epsilon_0(\epsilon_{obj}(\boldsymbol{r'}) - \epsilon_b(\boldsymbol{r'}))\boldsymbol{E}^N_{obj}(\boldsymbol{r'}) \tag{2}$$

If we want to use the scattered field at antenna M in $\hat{\boldsymbol{p}}$ direction, then we should also excite a test point source $\boldsymbol{J}^M_s(\boldsymbol{r})$ at antenna M in $\hat{\boldsymbol{p}}$ direction.

$$\boldsymbol{J}^M_s(\boldsymbol{r}) = I\hat{\boldsymbol{p}}\delta(\boldsymbol{r}) \tag{3}$$

Then, the numerical Green's function to link the scattered field at antenna M when transmitting from antenna N and for a given object's dielectric property is:

$$E^{\hat{p}}_{scat}(\boldsymbol{r}) = \frac{j\omega\epsilon_0}{I\delta(\boldsymbol{r})} \int_{V'} (\epsilon_{obj}(\boldsymbol{r'}) - \epsilon_b(\boldsymbol{r'}))\boldsymbol{E}^N_{obj}(\boldsymbol{r'})\boldsymbol{E}^M_{inc}(\boldsymbol{r'})dv' \tag{4}$$

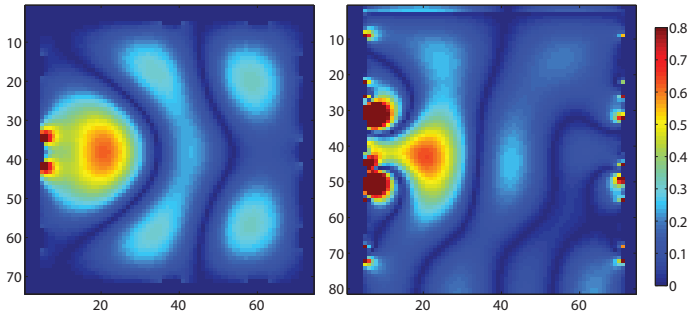

Fig. 4: $|Re(E_z)|$ Due to Single Transmitting Antenna at Resonance. (Left) Top View of Horizontal Cut (xy) Through Cavity, (Right) Side View of Vertical Cut (xz) Through Cavity

III. Results

A. Conformal FDTD Solver Results

Here in Figure 4, we show two slices of the magnitude of the vertical component of the electric field inside the imaging cavity (shown in Figure 1) due to a single transmit antenna at resonance. These fields are in agreement with results obtained previously from both CST Microwave Studio and Ansys HFSS, and are currently being used in tests of the inversion algorithm described in the methods section and outlined in Figure 2.

B. Numerical Green's Function

To validate the numerical Green's function, we place a cubic object with dielectric constant of 16 and size 4x4x4 cm^3 in the bottom center of the cubic imaging cavity consisting of 4 panels. The imaging cavity is filled with a coupling medium with a dielectric constant of 22. The transmitting antenna is located at the middle of one panel and the receiving antenna is at the bottom middle of the adjacent panel. A comparison of the scattered field S-parameters calculated by CST Microwave Studio and those estimated by the numerical Green's function method are shown in Figure 5. As can be seen from the figure, the scattered fields estimated by the numerical Green's function agree very well with those calculated by CST.

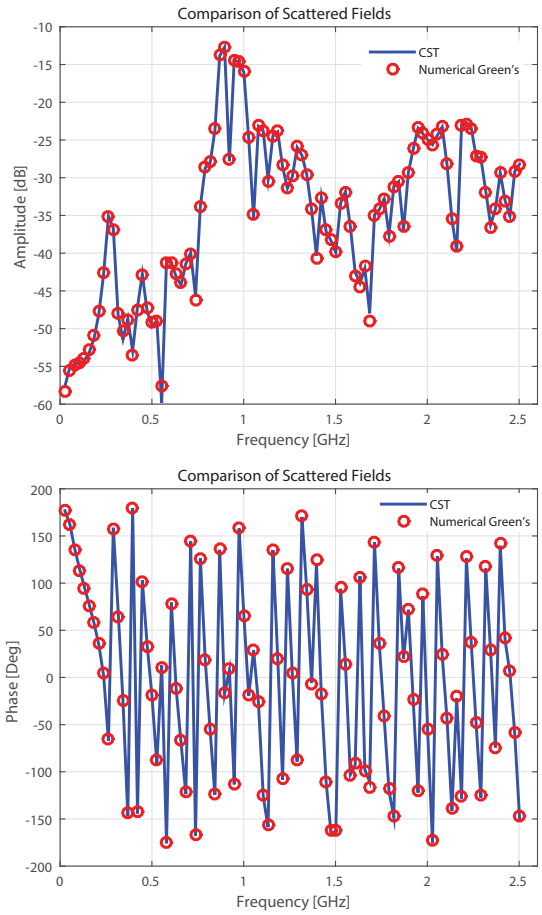

Fig. 5: Scattered fields comparison between FDTD solver and numerical Green's function estimation. Magnitudes agree within a mean absolute difference of 0.2 dB. Phases agree within a mean absolute difference of 2 degrees.

IV. Conclusion

With both the CFDTD solver and the integrated numerical Green's function validated through comparison with CST Microwave Studio, these methods are currently being used in ongoing microwave imaging experiments for both dielectric reconstruction and real-time thermal monitoring. In addition, the developed CFDTD method is CUDA-enabled, and tests are underway of the computational gains offered from GPU acceleration of the forward solver. Last, the authors would like to thank Maksym Tsvetkov for his assistance in hardware development and testing.

References

[1] M. Haynes, J. Stang, and M. Moghaddam, "Real-time Microwave Imaging of Differential Temperature for Thermal Therapy Monitoring," *IEEE Transactions on Biomedical Engineering*, vol. 61, pp. 1787–1797, June 2014.

[2] M. Haynes and M. Moghaddam, "Vector Green's function for S-parameter measurements of the electromagnetic volume integral equation," in *2011 IEEE International Symposium on Antennas and Propagation (APSURSI)*, pp. 1100–1103, July 2011.

[3] M. Haynes, J. Stang, and M. Moghaddam, "Microwave Breast Imaging Prototype with Integrated Numerical Characterization, *International Journal of Biomedical Imaging, Special Issue on Microwave Imaging and Emerging Applications*," vol. 2012, Jan. 2012.

[4] K. Yee, "Numerical Solution of Initial Boundary Value Problems Involving Maxwell's Equations in Isotropic Media," *IEEE Transactions on Antennas and Propagation*, vol. 14, pp. 302–307, May 1966.

[5] S. Benkler, N. Chavannes, and N. Kuster, "FDTD Subcell Models Powering Computational Antenna Optimization," in *The Second European Conference on Antennas and Propagation, 2007. EuCAP 2007*, pp. 1–4, Nov. 2007.

[6] M. Yuan and Q. H. Liu, "The Diagonal Tensor Approximation (DTA) for Objects in a Non-Canonical Inhomogeneous Background," *Progress In Electromagnetics Research*, vol. 112, pp. 1–21, 2011.

[7] G. Chen, J. Stang and M. Moghaddam, "A Conformal FDTD Method with Accurate Waveport Excitation and S-Parameter Extraction," *IEEE Trans. Antennas Propag.*, submitted Oct 5th, 2015, *in review.*